Weierstraß-Institut

für Angewandte Analysis und Stochastik

Leibniz-Institut im Forschungsverbund Berlin e. V.

Preprint ISSN 2198-5855

Guaranteed energy error estimators for a modified robust Crouzeix-Raviart Stokes element

Alexander Linke[1], Christian Merdon[1]

submitted: July 11, 2014

[1] Weierstrass Institute
Mohrenstr. 39
10117 Berlin
Germany
email: Alexander.Linke@wias-berlin.de
Christian.Merdon@wias-berlin.de

No. 1979

Berlin 2014

2010 *Mathematics Subject Classification.* 65N30, 65N15, 76D07.

Key words and phrases. mixed finite elements, a posteriori error estimation, divergence-free method, incompressible Stokes equations, Crouzeix-Raviart element.

Edited by
Weierstraß-Institut für Angewandte Analysis und Stochastik (WIAS)
Leibniz-Institut im Forschungsverbund Berlin e. V.
Mohrenstraße 39
10117 Berlin
Germany

Fax: +49 30 20372-303
E-Mail: preprint@wias-berlin.de
World Wide Web: http://www.wias-berlin.de/

Abstract. This paper provides guaranteed upper energy error bounds for a modified lowest-order nonconforming Crouzeix-Raviart finite element method for the Stokes equations. The modification from [A. Linke 2014, *On the role of the Helmholtz-decomposition in mixed methods for incompressible flows and a new variational crime*] is based on the observation that only the divergence-free part of the right-hand side should balance the vector Laplacian. The new method has optimal energy error estimates and can lead to errors that are smaller by several magnitudes, since the estimates are *pressure-independent*. An efficient a posteriori velocity error estimator for the modified method also should involve only the divergence-free part of the right-hand side. Some designs to approximate the Helmholtz projector are compared and verified by numerical benchmark examples. They show that guaranteed error control for the modified method is possible and almost as sharp as for the unmodified method.

1. Introduction

In the finite element analysis for the Stokes equations

$$-\operatorname{div}(\nu\nabla\mathbf{u}) + \nabla p = \mathbf{f}, \quad \nabla\cdot\mathbf{u} = 0, \tag{1}$$

the recent advance of [Lin14, BLMS14] led to a modified Crouzeix-Raviart nonconforming finite element method with an optimal and pressure-independent a priori estimate for the velocity in the broken energy norm $|||\cdot|||_{\mathrm{NC}}$ (see (7) below), i.e.,

$$|||\mathbf{u}-\mathbf{u}_h|||_{\mathrm{NC}} \le C \inf_{\mathbf{w}_h\in \mathrm{CR}(\mathcal{T})} |||\mathbf{u}-\mathbf{w}_h|||_{\mathrm{NC}}. \tag{2}$$

Taken such an pressure-independent estimate as a definition for a divergence-free method, the key ingredient in the design of divergence-free methods are divergence-free test functions. For the Crouzeix-Raviart finite element method, a simple reconstruction operator $\boldsymbol{\pi}^{\mathrm{RT}}$ maps the only discretely divergence-free test functions to divergence-free Raviart-Thomas test functions only in the right hand side, i.e. $\int_\Omega \mathbf{f}\cdot\mathbf{v}_h\,d\mathbf{x}$ is replaced by $\int_\Omega \mathbf{f}\cdot(\boldsymbol{\pi}^{\mathrm{RT}}\mathbf{v}_h)\,d\mathbf{x}$. This modification enables (2), while preserving optimal convergence rates. A more sophisticated reconstruction with BDM finite element functions was analysed in [BLMS14].

A posteriori error estimates for the standard Crouzeix-Raviart finite element method are well-known [DA05, CM14, BW91, Ver89, Ain04, VHS11, Ago94, DM98]. The ones compared in [CM14] are all of the form

$$|||\mathbf{u}-\mathbf{u}_h|||_{\mathrm{NC}}^2 \le \eta^2 + \gamma(\mathbf{v})^2$$

with some explicit part $\eta \approx \left\|\nu^{-1/2}h_{\mathcal{T}}\mathbf{f}\right\|_{L^2(\Omega)}$ and some conforming interpolation error contribution $\gamma(\mathbf{v}) := |||\mathbf{u}_h-\mathbf{v}|||_{\mathrm{NC}} + c_0^{-1}\left\|\nu^{1/2}\operatorname{div}\mathbf{v}\right\|_{L^2(\Omega)}$ that includes the inf-sup constant c_0. However, the estimation by the term η is not robust against ν for the modified Crouzeix-Raviart finite element method at hand for the following fact. Opposite to the standard

Date: 3rd July 2014.

method, for discretely divergence-free test functions $\mathbf{v}_h$, the velocity reconstructions $\boldsymbol{\pi}^{\mathrm{RT}}\,\mathbf{v}_h$ are divergence-free and satisfy

$$\int_\Omega \mathbf{f}\cdot(\boldsymbol{\pi}^{\mathrm{RT}}\,\mathbf{v}_h)\,d\mathbf{x} = \int_\Omega (\mathbf{f}-\nabla w)\cdot(\boldsymbol{\pi}^{\mathrm{RT}}\,\mathbf{v}_h)\,d\mathbf{x} \quad \text{for all } w\in H^1(\Omega). \tag{3}$$

In fact, only the Helmholtz projector of $\mathbf{f}$, i.e. the divergence-free part of its Helmholtz decomposition, is needed in the a posteriori error estimate and has to be approximated efficiently by some $w\in H^1(\Omega)$. This approximation enters the new error estimator for the modified Crouzeix-Raviart method through the term $\mu(w) := C_F\big\|\nu^{-1/2}h_{\mathcal{T}}(\mathbf{f}-\nabla w)\big\|_{L^2(\Omega)}$ and replaces η. The crucial part for the efficiency of the estimator is a good approximation of the minimiser of $\mu(w)$ amongst $w\in H^1(\Omega)$ which may stem from conforming finite element solutions of a related scalar Poisson problem.

Instead, the standard Crouzeix-Raviart finite element method and its a posteriori error estimates cannot exploit this fact, because the test functions are not divergence-free and so do not allow for (3).

The remaing parts of the paper are outlined as follows. Section 2 explains the setting for the continuous problem and its finite element approximation with the standard and the modified Crouzeix-Raviart finite element method. Section 3 recalls guaranteed upper bounds for the standard Crouzeix-Raviart finite element method in the energy norm and derives guaranteed upper bounds also for the modified method. Section 4 explains efficient realisations of the guaranteed upper bounds, in particular for the design of w in (3). Section 5 reports on some numerical examples to validate the efficiency and robustness of the new guaranteed upper bounds.

Throughout this paper, standard notation and Sobolev spaces $V := H^1_0(\Omega)^d$, $H(\mathrm{div},\Omega)$ and $Q := L^2_0(\Omega)$ are employed.

2. Continuous and discrete setting

This section explains the continuous and the discrete setting for the model problem under consideration.

2.1. Continuous setting.

The weak solution $(\mathbf{u},p)\in V\times Q$ of the continuous steady incompressible Stokes problem satisfies the equations

$$\begin{aligned} a(\mathbf{u},\mathbf{v})+b(\mathbf{v},p) &= F(\mathbf{v}),\\ b(\mathbf{u},q) &= 0 \qquad \text{for all } (\mathbf{v},q)\in V\times Q \end{aligned} \tag{4}$$

with the multilinear forms defined by

$$\begin{aligned} a: V\times V\to\mathbb{R}, &\qquad a(\mathbf{u},\mathbf{v}) := \int_\Omega \nu\nabla\mathbf{u}:\nabla\mathbf{v}\,d\mathbf{x},\\ b: V\times Q\to\mathbb{R}, &\qquad b(\mathbf{u},q) := -\int_\Omega q\,\mathrm{div}\,\mathbf{u}\,d\mathbf{x},\\ F: V\to\mathbb{R}, &\qquad F(\mathbf{v}) := \int_\Omega \mathbf{f}\cdot\mathbf{v}\,d\mathbf{x}. \end{aligned}$$

Within the set of weakly differentiable, divergence-free functions

$$V_0 := \{\mathbf{v}\in V : \mathrm{div}\,\mathbf{v}=0\}, \tag{5}$$

the saddle point problem (4) can be rewritten into an elliptic problem for the velocity alone, i.e., $\mathbf{u}\in V_0$ such that

$$a(\mathbf{u},\mathbf{v}) = F(\mathbf{v}) \qquad \text{for all } \mathbf{v}\in V_0. \tag{6}$$

2.2. **Notation.** In the following, $\mathcal{T}$ denotes a regular triangulation of the domain Ω into triangles ($d = 2$) or tetrahedra ($d = 3$) with simplex faces $\mathcal{E}$ and nodes $\mathcal{N}$. The subset $\mathcal{E}(\Omega)$ denotes the set of interior faces, while $\mathcal{E}(\partial\Omega)$ denotes the set of faces along the domain boundary $\partial\Omega$. For any element $T \in \mathcal{T}$, $\mathrm{mid}(T)$ denotes the barycenter of T. Likewise, $\mathrm{mid}(F)$ denotes the barycenter of a face $F \in \mathcal{E}$, and $\mathbf{n}_F$ abbreviates a face normal vector.

The function space of $P_k(\mathcal{T})$ contains piecewise polynomials of order k with respect to $\mathcal{T}$. The space of Crouzeix-Raviart velocity trial functions is given by

$$\mathrm{CR}(\mathcal{T}) := \big\{\mathbf{v}_h \in P_1(\mathcal{T})^d \,\big|\, \text{for all } T \in \mathcal{T},\ [\mathbf{v}_h](\mathrm{mid}(F)) = \mathbf{0} \text{ for all } F \in \mathcal{E}(\Omega) \\ \&\ \mathbf{v}_h(\mathrm{mid}(F)) = \mathbf{0} \text{ for all } F \in \mathcal{E}(\partial\Omega)\big\}$$

and the discrete pressure trial function space reads

$$Q(\mathcal{T}) := \left\{ q_h \in P_0(\mathcal{T}) : \int_\Omega q_h \, d\mathbf{x} = 0 \right\}.$$

Furthermore, the set of lowest order Raviart-Thomas finite element functions reads

$$\mathrm{RT}(\mathcal{T}) := \Big\{\mathbf{v}_h \in P_1(\mathcal{T})^d \cap H(\mathrm{div},\Omega) \,\Big|\, \forall T \in \mathcal{T}\ \exists \mathbf{a}_T \in \mathbb{R}^d, b_T \in \mathbb{R},\ \mathbf{v}_h|_T(\mathbf{x}) = \mathbf{a}_T + b_T\mathbf{x}\Big\}.$$

Note, that any Raviart-Thomas function is uniquely defined by its constant normal fluxes at the face barycenters [BF91].

The discrete setting employs the *broken gradient* $\nabla_h : V \oplus \mathrm{CR}(\mathcal{T}) \to L^2(\Omega)^{d\times d}$ and the *broken divergence* $\nabla_h \cdot (\cdot) : V \oplus \mathrm{CR}(\mathcal{T}) \to L^2(\Omega)$ in the sense that

$$(\nabla_h \mathbf{v}_h)|_T := \nabla(\mathbf{v}_h|_T), \quad (\nabla_h \cdot \mathbf{v}_h)|_T := \mathrm{div}(\mathbf{v}_h|_T) \quad \text{for all } T \in \mathcal{T}.$$

The discrete energy norm for the space $V \oplus \mathrm{CR}(\mathcal{T})$ reads

$$|||\mathbf{v}_h|||_{\mathrm{NC}} := \left(\int_\Omega \nu \nabla_h \mathbf{v}_h : \nabla_h \mathbf{v}_h \, d\mathbf{x}\right)^{1/2} = \big\|\nu^{1/2}\nabla_h \mathbf{v}_h\big\|_{L^2(\Omega)}. \tag{7}$$

2.3. **Interpolation operators.** The Crouzeix-Raviart interpolation operator $\boldsymbol{\pi}^{\mathrm{CR}} : V \oplus \mathrm{CR}(\mathcal{T}) \to \mathrm{CR}(\mathcal{T})$ is given by

$$(\boldsymbol{\pi}^{\mathrm{CR}}\,\mathbf{v})(\mathrm{mid}(F)) = \frac{1}{|F|}\int_F \mathbf{v}\, ds \quad \text{for all } F \in \mathcal{E}.$$

The Raviart-Thomas interpolation operator $\boldsymbol{\pi}^{\mathrm{RT}} : V \oplus \mathrm{CR}(\mathcal{T}) \to \mathrm{RT}(\mathcal{T})$ is defined by

$$\mathbf{n}_F \cdot (\boldsymbol{\pi}^{\mathrm{RT}}\,\mathbf{v})(\mathrm{mid}(F)) = \frac{1}{|F|}\int_F \mathbf{v}\cdot\mathbf{n}_F\, ds \quad \text{for all } F \in \mathcal{E}.$$

Note that, due to continuity in the face barycenters, this is well-defined also for $\mathbf{v} \in \mathrm{CR}(\mathcal{T})$.

By Gauss' theorem, it immediately follows, for any $\mathbf{v} \in V_0$, that $\mathrm{div}\,\boldsymbol{\pi}^{\mathrm{RT}}\,\mathbf{v} = 0$ and $\nabla_h \cdot \boldsymbol{\pi}^{\mathrm{CR}}\,\mathbf{v} = 0$. Morevoer, there are the stability and approximation properties

$$|||\,\boldsymbol{\pi}^{\mathrm{CR}}\,\mathbf{v}|||_{\mathrm{NC}} \le |||\mathbf{v}|||_{\mathrm{NC}} \quad \text{for all } v \in V, \tag{8}$$

$$\big\|\mathbf{v} - \boldsymbol{\pi}^{\mathrm{CR}}\,\mathbf{v}\big\|_{L^2(\Omega)} \le C\big\|h_{\mathcal{T}}\nabla(\mathbf{v} - \boldsymbol{\pi}^{\mathrm{CR}}\,\mathbf{v})\big\|_{L^2(\Omega)} \quad \text{for all } v \in V, \tag{9}$$

$$\big\|\mathbf{v} - \boldsymbol{\pi}^{\mathrm{RT}}\,\mathbf{v}\big\|_{L^2(\Omega)} \le C_F\big\|h_{\mathcal{T}}\nabla\mathbf{v}\big\|_{L^2(\Omega)} \quad \text{for all } v \in V \cup \mathrm{CR}(\mathcal{T}), \tag{10}$$

where the generic constants C and C_F depend only on the shape of the simplices in the triangulation $\mathcal{T}$ but not on their size [BF91, AD99, CGR12]. Explicit upper bounds for the Fortin-interpolation C_F constant can be found in [CGR12] and its proof extends to functions $v \in \mathrm{CR}(\mathcal{T})$. For right-isosceles triangles they compute $C_F \le 0.6215$.

2.4. **Standard and modified Crouzeix-Raviart finite element method.** The discrete weak formulation of the model problem employs the two bilinear forms

$$a_h : \mathrm{CR}(\mathcal{T}) \times \mathrm{CR}(\mathcal{T}) \to \mathbb{R}, \qquad a_h(\mathbf{u}_h, \mathbf{v}) := \int_\Omega \nu \nabla_h \mathbf{u}_h : \nabla_h \mathbf{v}_h \, d\mathbf{x},$$
$$b_h : \mathrm{CR}(\mathcal{T}) \times Q \to \mathbb{R}, \qquad b_h(\mathbf{u}_h, q_h) := -\int_\Omega q_h \nabla_h \cdot \mathbf{u}_h \, d\mathbf{x}.$$

Given one of the two interpolation operators above, i.e. $\boldsymbol{\pi}^{\mathrm{div}} \in \{\boldsymbol{\pi}^{\mathrm{CR}}, \boldsymbol{\pi}^{\mathrm{RT}}\}$, the discrete Stokes problem seeks $(\mathbf{u}_h, p_h) \in \mathrm{CR}(\mathcal{T}) \times Q(\mathcal{T})$ such that

$$\begin{aligned} a_h(\mathbf{u}_h, \mathbf{v}_h) + b_h(\mathbf{v}, p_h) &= F(\boldsymbol{\pi}^{\mathrm{div}} \mathbf{v}_h), \\ b_h(\mathbf{u}_h, q_h) &= 0 \qquad \text{for all } (\mathbf{v}_h, q_h) \in \mathrm{CR}(\mathcal{T}) \times Q(\mathcal{T}). \end{aligned} \tag{11}$$

The choice $\boldsymbol{\pi}^{\mathrm{div}} = \boldsymbol{\pi}^{\mathrm{CR}}$ leads to the classical Crouzeix-Raviart nonconforming finite element method in the spirit of [CR73], while $\boldsymbol{\pi}^{\mathrm{div}} = \boldsymbol{\pi}^{\mathrm{RT}}$ constitutes the variational crime suggested in [Lin14] that maps discretely divergence-free test functions to divergence-free functions in $H(\mathrm{div}, \Omega)$. As shown in [Lin14, BLMS14], this modification allows an optimal pressure-independent a priori energy error estimate in the form

$$|||\mathbf{u} - \mathbf{u}_h|||_{\mathrm{NC}} \leq C \inf_{\mathbf{w}_h \in \mathrm{CR}(\mathcal{T})} |||\mathbf{u} - \mathbf{w}_h|||_{\mathrm{NC}}.$$

Remark 1 (BDM reconstructions)**.** *The BDM reconstruction* $\boldsymbol{\pi}^{\mathrm{div}} = \boldsymbol{\pi}^{\mathrm{BDM}}$ *from* [BLMS14] *into the Brezzi-Douglas-Marini finite element space*

$$\mathrm{BDM}(\mathcal{T}) := \left\{ \mathbf{v}_h \in P_1(\mathcal{T})^d : [\mathbf{v}_h \cdot \mathbf{n}_E] = 0 \text{ along all } E \in \mathcal{E} \right\}$$

additionaly allows for a provable optimal L^2 *error convergence rate. The operator* $\boldsymbol{\pi}^{\mathrm{BDM}} : V \cup \mathrm{CR}(\mathcal{T}) \to \mathrm{BDM}(\mathcal{T})$ *is defined such that, for all* $p_h \in P_1(E)$ *on a face* $E \in \mathcal{E}$*,*

$$\int_E (\boldsymbol{\pi}^{\mathrm{BDM}} \mathbf{v}) \cdot \mathbf{n}_E \, p_h \, ds = \begin{cases} \int_E \{\{\mathbf{v} \cdot \mathbf{n_E}\}\} \, p_h \, ds & \text{for all } E \in \mathcal{E}(\Omega) \\ \int_E (\boldsymbol{\pi}^{\mathrm{RT}} \mathbf{v}) \cdot \mathbf{n}_E \, p_h \, ds & \text{for all } E \in \mathcal{E}(\partial\Omega). \end{cases}$$

Like the continuous incompressible Stokes equations, also the discretization (11) can be formulated as an elliptic problem [Tem91, GR86] within the space of discretely divergence-free functions

$$V_{0,h} := \{\mathbf{v}_h \in \mathrm{CR}(\mathcal{T}) : b(\mathbf{v}_h, q_h) = 0 \text{ for all } q_h \in Q(\mathcal{T})\} = \{\mathbf{v}_h \in \mathrm{CR}(\mathcal{T}) : \nabla_h \cdot \mathbf{v}_h = 0\}. \tag{12}$$

Then, $\mathbf{u}_h \in V_{0,h}$ is uniquely defined by

$$a_h(\mathbf{u}_h, \mathbf{v}_h) = F(\boldsymbol{\pi}^{\mathrm{div}} \mathbf{v}_h) \quad \text{for all } \mathbf{v}_h \in V_{0,h}. \tag{13}$$

3. A posteriori error estimates

This section recalls a posteriori error estimation results from [CM14, DA05] for $\boldsymbol{\pi}^{\mathrm{div}} = \boldsymbol{\pi}^{\mathrm{CR}}$ and derives improved results for the modified Crouzeix-Raviart finite element method for $\boldsymbol{\pi}^{\mathrm{div}} = \boldsymbol{\pi}^{\mathrm{RT}}$. The original estimate includes data oscillations

$$\mathrm{osc}(\mathbf{f}, \mathcal{T}) := \left\| h_{\mathcal{T}} (\mathbf{f} - \mathbf{f}_{\mathcal{T}}) \right\|_{L^2(\Omega)} \quad \text{with integral mean} \quad \mathbf{f}_{\mathcal{T}}|_T := \frac{1}{|T|} \int_T \mathbf{f} \, d\mathbf{x} \quad \text{for all } T \in \mathcal{T}$$

and the elementwise Poincaré constant $C_P(T) := \sup_{v \in V} \left\| v - v_T \right\|_{L^2(T)} / h_T |||v|||_{\mathrm{NC}}$. In 2D, [LS10] shows $C_P(T) = 1/j_{1,1}$ where $j_{1,1} = 3.8317\ldots$ is the first positive root of the first

Bessel function J_1. In 3D, the constant $C_P(T) = 1/\pi$ is valid for every convex domain [PW60, Beb03]. Both estimates depend on the inf-sup constant

$$0 < c_0 := \inf_{q\in Q\setminus\{0\}} \sup_{\mathbf{v}\in V\setminus\{0\}} \frac{\int_\Omega q \operatorname{div} \mathbf{v}\, d\mathbf{x}}{\|\nabla \mathbf{v}\|_{L^2(\Omega)} \|q\|_{L^2(\Omega)}}$$

and the contribution

$$\gamma(\mathbf{v}) := |||\mathbf{u}_h - \mathbf{v}|||_{\mathrm{NC}} + c_0^{-1} \left\|\nu^{1/2} \operatorname{div} \mathbf{v}\right\|_{L^2(\Omega)} \quad \text{for } \mathbf{v} \in H^1(\Omega;\mathbb{R}^d).$$

Theorem 1 (A posteriori error estimates for the standard Crouzeix-Raviart FEM, [CM14])**.** *For the solution* $\mathbf{u}_h$ *of* (11) *with* $\boldsymbol{\pi}^{\mathrm{div}} = \boldsymbol{\pi}^{\mathrm{CR}}$*, it holds*

$$|||\mathbf{e}|||_{NC}^2 \le \eta^2 + \min_{\substack{\mathbf{v}\in H^1(\Omega;\mathbb{R}^d)\\ \mathbf{v}=\mathbf{u}_D \text{ along } \partial\Omega}} \gamma(\mathbf{v})^2 \tag{14}$$

where $\eta := \left\|\nu^{-1/2}\mathbf{f}_{\mathcal{T}}/2 \otimes \mathbf{d}\right\|_{L^2(\Omega)} + C_P(\mathcal{T}) \operatorname{osc}(\nu^{-1/2}\mathbf{f}, \mathcal{T})$ *for the function* $\mathbf{d}(x)|_T := (\mathbf{x} - \operatorname{mid}(T))$ *for* $\mathbf{x} \in T \in \mathcal{T}$*.*

Here, $x \otimes y \in \mathbb{R}^{d\times d}$ denotes the dyadic product of two vectors $x, y \in \mathbb{R}^d$.

Proof. See [CM14]. □

Theorem 2 (A posteriori error estimates for the modified Crouzeix-Raviart FEM)**.** *For the solution* $\mathbf{u}_h$ *of* (11) *with* $\boldsymbol{\pi}^{\mathrm{div}} = \boldsymbol{\pi}^{\mathrm{RT}}$*, it holds*

$$|||\mathbf{e}|||_{NC}^2 \le \min_{w\in H^1(\Omega)} \mu(w)^2 + \min_{\substack{\mathbf{v}\in H^1(\Omega;\mathbb{R}^d)\\ \mathbf{v}=\mathbf{u}_D \text{ along } \partial\Omega}} \gamma(\mathbf{v})^2 \tag{15}$$

where $\mu(w) := C_F \left\|\nu^{-1/2} h_{\mathcal{T}} (\mathbf{f} - \nabla w)\right\|_{L^2(\Omega)}$*.*

Proof. As in the proof of Theorem 1 from [CM14], the point of departure is the orthogonal split

$$\nu\nabla_h \mathbf{e} = \nu\nabla \mathbf{z} + y$$

into $\mathbf{z} \in V_0$ with

$$\int_\Omega \nu\nabla \mathbf{z} : \nabla \mathbf{v}\, d\mathbf{x} = \int_\Omega \nu\nabla_h \mathbf{e} : \nabla \mathbf{v}\, d\mathbf{x} \quad \text{for all } \mathbf{v} \in V_0,$$

and the remainder

$$y \in Y := \left\{ y \in L^2(\Omega;\mathbb{R}^{d\times d}) \,\middle|\, \int_\Omega y : \nabla \mathbf{v}\, d\mathbf{x} = 0 \quad \text{for all } \mathbf{v} \in V_0 \right\}.$$

Orthogonality holds in the sense of

$$|||\mathbf{e}|||_{\mathrm{NC}}^2 = |||\mathbf{z}|||_{\mathrm{NC}}^2 + \left\|\nu^{-1/2} y\right\|_{L^2(\Omega)}^2 = \int_\Omega \nu\nabla_h \mathbf{e} : \nabla \mathbf{z}\, d\mathbf{x} + \int_\Omega \nabla_h \mathbf{e} : y\, d\mathbf{x}.$$

The estimate of $\int_\Omega \nu\nabla_h \mathbf{e} : \nabla \mathbf{z}\, d\mathbf{x}$ is different from the proof in [CM14]. Since $\int_T \nabla \mathbf{z}\, d\mathbf{x} = \int_T \nabla\, \boldsymbol{\pi}^{\mathrm{CR}}\, \mathbf{z}\, d\mathbf{x}$ (by an integration by parts) for all $T \in \mathcal{T}$, (11) for $\boldsymbol{\pi}^{\mathrm{div}} = \boldsymbol{\pi}^{\mathrm{RT}}$ shows

$$\int_\Omega \nu\nabla_h \mathbf{e} : \nabla \mathbf{z}\, d\mathbf{x} = \int_\Omega \mathbf{f} \cdot (\mathbf{z} - \boldsymbol{\pi}^{\mathrm{RT}}\, \mathbf{z})\, d\mathbf{x}.$$

Both functions $\mathbf{z}$ and $\boldsymbol{\pi}^{\mathrm{RT}}\,\mathbf{z}$ are divergence-free and have zero normal components along the boundary $\partial\Omega$ and therefore are orthogonal on any gradient ∇w of any $w \in H^1(\Omega)$. This and the Fortin interpolation estimate (10) yield

$$\begin{aligned}|||\mathbf{z}|||_{\mathrm{NC}}^2 = \int_\Omega \nu\nabla_h\mathbf{e} : \nabla\mathbf{z}\,d\mathbf{x} &= \int_\Omega (\mathbf{f}-\nabla w)\cdot(\mathbf{z}-\boldsymbol{\pi}^{\mathrm{RT}}\,\mathbf{z})\,d\mathbf{x}\\ &\le \big\|\mathbf{f}-\nabla w\big\|_{L^2(\Omega)}\big\|\mathbf{z}-\boldsymbol{\pi}^{\mathrm{RT}}\,\mathbf{z}\big\|_{L^2(\Omega)}\\ &\le C_F\big\|\nu^{-1/2}h_{\mathcal{T}}(\mathbf{f}-\nabla w)\big\|_{L^2(\Omega)}|||\mathbf{z}|||_{\mathrm{NC}}.\end{aligned}$$

In total

$$|||\mathbf{z}|||_{\mathrm{NC}} \le C_F \min_{w\in H_0^1(\omega)}\big\|\nu^{-1/2}h_{\mathcal{T}}(\mathbf{f}-\nabla w)\big\|_{L^2(\Omega)}.$$

It remains to estimate $\int_\Omega \nabla_h\mathbf{e} : y\,d\mathbf{x}$ as in [DA05, CM14]. The theory of [Gal94, Chapter III.1] shows that, for each $y \in Y$, there exists some $w \in L^2_0(\Omega) := \{q \in L^2(\Omega) \,\big|\, \int_\Omega q\,d\mathbf{x} = 0\}$ with

$$\int_\Omega y : \nabla\mathbf{v}\,d\mathbf{x} = \int_\Omega w\,\mathrm{div}\,\mathbf{v}\,d\mathbf{x} \quad \text{for all } \mathbf{v}\in V \tag{16}$$

and

$$\big\|w\big\|_{L^2(\Omega)} \le c_0^{-1}\,\big\|y\big\|_{L^2(\Omega)}.$$

Hence, given any $\mathbf{v} \in H^1(\Omega;\mathbb{R}^d)$ with $\mathbf{u}-\mathbf{v}=0$ on $\partial\Omega$, it holds

$$\begin{aligned}\big\|\nu^{-1/2}y\big\|_{L^2(\Omega)}^2 &= \int_\Omega \nabla_h\mathbf{e} : y\,d\mathbf{x}\\ &= \int_\Omega \nu^{1/2}\nabla_h(\mathbf{u}_h-\mathbf{v}) : \nu^{-1/2}y\,d\mathbf{x} + \int_\Omega \nabla(\mathbf{v}-\mathbf{u}) : y\,d\mathbf{x}\\ &\le |||\mathbf{u}_h-\mathbf{v}|||_{\mathrm{NC}}\big\|\nu^{-1/2}y\big\|_{L^2(\Omega)} + \int_\Omega \mathrm{div}(\mathbf{v}-\mathbf{u})w\,d\mathbf{x}\\ &\le \Big(|||\mathbf{u}_h-\mathbf{v}|||_{\mathrm{NC}} + c_0^{-1}\big\|\nu^{1/2}\,\mathrm{div}\,\mathbf{v}\big\|_{L^2(\Omega)}\Big)\,\big\|\nu^{-1/2}y\big\|_{L^2(\Omega)}.\end{aligned}$$

The combination of all mentioned results concludes the proof. □

Remark 2 (Efficiency of $\mu(w)$)**.** *For $w \equiv 0$, it holds $\mu(0) \approx \big\|h_{\mathcal{T}}\mathbf{f}\big\|_{L^2(\Omega)} \approx \eta$ up to higher-order terms. Hence, $\mu(0)$ is as efficient as η. Behind the minimisation of $\mu(w) = \big\|\mathbf{f}-\nabla w\big\|_{L^2(\Omega)}$ is in fact an approximation of the L^2 norm of the divergence-free part of the Helmholtz decomposition*

$$\nu^{-1}\mathbf{f} = \nu^{-1}\nabla\alpha + \beta \tag{17}$$

into $\alpha \in H^1(\Omega)/\mathbb{R}$ and $\beta \in H^1(\mathrm{div},\Omega)$ with $\nabla\cdot\beta = 0$ in Ω and $(\mathbf{f}-\nabla\alpha)\cdot\mathrm{n} = 0$ along $\partial\Omega$. Every approximation w of α gives an upper bound in the sense

$$\big\|\nu^{-1/2}(\mathbf{f}-\nabla w)\big\|_{L^2(\Omega)}^2 = \big\|\nu^{-1/2}\nabla(\alpha-w)\big\|_{L^2(\Omega)}^2 + \big\|\nu^{1/2}\beta\big\|_{L^2(\Omega)}^2 \ge \big\|\nu^{1/2}\beta\big\|_{L^2(\Omega)}^2. \tag{18}$$

Therefore,

$$\min_{w\in H^1(\Omega)}\mu(w) = \mu(\alpha) = C_F\big\|h_{\mathcal{T}}\nu^{1/2}\beta\big\|_{L^2(\Omega)}.$$

Thus, $\mu(w)$ has the potential to be more efficient than η for right-hand sides $\mathbf{f}$ with a large irrotational component and this is exactly the case the modified Crouzeix-Raviart method is designed for. To make the efficiency of the a posteriori error estimator robust against this

contribution, a good approximation of α by w is needed. Possible designs are suggested in Section 4.2.

4. Suitable interpolations for the design of upper bounds

The guaranteed upper bounds from Theorem 2 need efficient designs of two conforming interpolations $\mathbf{v} \in H^1(\Omega;\mathbb{R}^d)$ and $w \in H^1(\Omega)$. The first interpolation $\mathbf{v}$ needs to be close to $\mathbf{u}_h$ in the energy norm and the second interpolation w needs to be close to α from the Helmholtz decomposition (17) of $\mathbf{f}$ as pointed out in Remark 2. Possible designs for $\mathbf{v}$ were studied in [CM14], whereas designs for w are open.

4.1. Designs for $\gamma(\mathbf{v})$.

Since we want to concentrate on the new error estimator contribution μ, we stick to the error estimators for the second contribution that were the most efficient in the comparison of [CM14]. Algorithm 1 computes the global minimisers $\mathbf{v}_{\mathrm{MP1}}$ in $P_1(\mathcal{T})\cap C(\Omega)$, $\mathbf{v}_{\mathrm{MP2}}$ in $P_2(\mathcal{T})\cap C(\Omega)$ and $\mathbf{v}_{\mathrm{MP1red}}$ in $P_1(\mathrm{red}(\mathcal{T}))\cap C(\Omega)$ on the red-refined triangulation $\mathrm{red}(\mathcal{T})$.

The idea behind Algorithm 1 is the argument

$$(|a|+|b|)^2 = \min_{\lambda\in\mathbb{R}_+}\left((1+\lambda)\,|a|^2+(1+1/\lambda)\,|b|^2\right) \quad \text{for any } (a,b)\in\mathbb{R}^2$$

with minimum $\lambda = |b|\,/\,|a|$. Hence, for any $W(\mathcal{T})\subseteq H^1(\Omega)$,

$$\begin{aligned}&\operatorname*{argmin}_{\mathbf{v}\in W(\mathcal{T})}\left(|||\mathbf{u}_h-\mathbf{v}|||_{\mathrm{NC}}+\left\|\nu^{1/2}\operatorname{div}\mathbf{v}\right\|_{L^2(\Omega)}\right)^2\\ &\qquad=\operatorname*{argmin}_{\mathbf{v}\in W(\mathcal{T})}\min_{\lambda\in\mathbb{R}_+}\left((1+\lambda)|||\mathbf{u}_h-\mathbf{v}|||_{\mathrm{NC}}^2+(1+1/\lambda)\left\|\nu^{1/2}\operatorname{div}\mathbf{v}\right\|_{L^2(\Omega)}^2/c_0^2\right)\end{aligned}$$

Algorithm 1 alternately computes the minimiser $\mathbf{v}_{W(\mathcal{T})}$ (for a fixed λ) and the minimal λ (for a fixed $\mathbf{v}_{W(\mathcal{T})}$). In this way, the right hand side is minimised in each step and converges to the minimum. Undisplayed experiments convey that three iterations give satisfactory results.

Algorithm 1: Minimisation of γ

Input : $\mathbf{u}_h\in\mathrm{CR}(\mathcal{T})$, $W(\mathcal{T})\in\{P_1(\mathcal{T})\cap C(\Omega), P_1(\mathrm{red}(\mathcal{T}))\cap C(\Omega), P_2(\mathcal{T})\cap C(\Omega)\}$

Output: $v_{\mathrm{MP1}} := v_{P_1(\mathcal{T})\cap C(\Omega)}$, $v_{\mathrm{MP1red}} := v_{P_1(\mathrm{red}(\mathcal{T}))\cap C(\Omega)}$, or $v_{\mathrm{MP2}} := v_{P_2(\mathcal{T})\cap C(\Omega)}$

Set $\lambda := 1$

for $\ell = 1,2,3$ **do**

Compute the minimiser

$$\mathbf{v}_{W(\mathcal{T})} := \operatorname*{argmin}_{\mathbf{v}\in W(\mathcal{T})}\left((1+\lambda)|||\mathbf{u}_h-\mathbf{v}|||_{\mathrm{NC}}^2+(1+1/\lambda)\left\|\nu^{1/2}\operatorname{div}\mathbf{v}\right\|_{L^2(\Omega)}^2/c_0^2\right) \tag{19}$$

Update $\lambda := \left\|\nu^{1/2}\operatorname{div}\mathbf{v}_{W(\mathcal{T})}\right\|_{L^2(\Omega)}/\left(c_0|||\mathbf{u}_h-\mathbf{v}_{W(\mathcal{T})}|||_{\mathrm{NC}}\right)$

end

This results in the three error estimators

$$\begin{aligned}\eta_{\mathrm{MP1}}^2 &:= \eta^2+\gamma(v_{\mathrm{MP1}})^2,\\ \eta_{\mathrm{MP1red}}^2 &:= \eta^2+\gamma(v_{\mathrm{MP1red}})^2,\\ \eta_{\mathrm{MP2}}^2 &:= \eta^2+\gamma(v_{\mathrm{MP2}})^2.\end{aligned}$$

All of them are guaranteed upper bounds of the energy error $|||\mathbf{u}-\mathbf{u}_h|||_{\mathrm{NC}}$ for the standard Crouzeix-Raviart finite element method (11) for $\boldsymbol{\pi}^{\mathrm{div}}=\boldsymbol{\pi}^{\mathrm{CR}}$ in the sense of Theorem 1.

Remark 3. *To reduce the computational costs of* (19) *one might use the nodal interpolation* v_{MAred} *from* [CM14] *as an initial guess for a preconditioned conjugate gradients scheme with Jacobi preconditioner to draw near the minimiser of* (19) *for* $W(\mathcal{T})=P_1(\mathrm{red}(\mathcal{T}))\cap C(\Omega)$. *Similarly, the nodal values of* $\mathbf{v}_{MAred}$ *define some piecewise quadratic function and hence an initial value for some PCG algorithm for the approximation of the minimiser of* (19) *for* $W(\mathcal{T})=P_2(\mathcal{T})\cap C(\Omega)$.

4.2. **Designs for $\mu(w)$.** The function α from (17) satisfies the scalar Poisson equation

$$\mathrm{div}(\nu^{-1}\nabla\alpha)=\mathrm{div}(\nu^{-1}\mathbf{f}) \quad \text{and} \quad (\mathbf{f}-\nabla\alpha)\cdot\mathrm{n}=0 \text{ along } \partial\Omega$$

with its weak formulation

$$\begin{aligned}\int_\Omega \nu^{-1}\nabla\alpha\cdot\nabla v\,d\mathbf{x} &= -\int_\Omega \mathrm{div}(\nu^{-1}\mathbf{f})v\,d\mathbf{x}-\int_{\partial\Omega}(\mathbf{f}\cdot\mathrm{n})v\,d\mathbf{x}\\ &=\int_\Omega \nu^{-1}\mathbf{f}\cdot\nabla v\,d\mathbf{x} \quad \text{for all } v\in H^1(\Omega)/\mathbb{R}.\end{aligned} \tag{20}$$

To approximate α one can solve (20) by conforming $P_k(\mathcal{T})\cap H^1(\Omega)/\mathbb{R}$ finite element methods. If such a method satisfies (and this is true for smooth data and domain or adaptive mesh refinement) $\|\nu^{-1/2}\nabla(\alpha-w)\|_{L^2(\Omega)}\lesssim h^k\|\nu^{-1/2}\,\mathrm{div}\,\mathbf{f}\|_{L^2(\Omega)}$, (18) shows

$$\begin{aligned}\mu(w)^2=C_F^2\|\nu^{-1/2}h_{\mathcal{T}}(\mathbf{f}-\nabla w)\|^2_{L^2(\Omega)} &\le h^2C_F^2\left(\|\nu^{-1/2}\nabla(\alpha-w)\|^2_{L^2(\Omega)}+\|\nu^{1/2}\beta\|^2_{L^2(\Omega)}\right)\\ &\lesssim C_F^2\left(h^{2+2k}\|\nu^{-1/2}\,\mathrm{div}\,\mathbf{f}\|_{L^2(\Omega)}+h^2\|\nu^{1/2}\beta\|^2_{L^2(\Omega)}\right).\end{aligned}$$

Then, $\mu(w)$ converges to $C_Fh\|\nu^{1/2}\beta\|_{L^2(\Omega)}\le C_Fh\|\nu^{1/2}\Delta\mathbf{u}\|_{L^2(\Omega)}$ with at least quadratic speed. The numerical examples below compare the three estimators

$$\begin{aligned}\widehat{\eta}^2_{\mathrm{MP1}}&:=\min_{w\in P_1(\mathcal{T})\cap H^1(\Omega)/\mathbb{R}}\mu(w)^2+\gamma(v_{\mathrm{MP1}})^2,\\ \widehat{\eta}^2_{\mathrm{MP1red}}&:=\min_{w\in P_1(\mathrm{red}(\mathcal{T}))\cap H^1(\Omega)/\mathbb{R}}\mu(w)^2+\gamma(v_{\mathrm{MP1red}})^2,\\ \widehat{\eta}^2_{\mathrm{MP2}}&:=\min_{w\in P_2(\mathcal{T})\cap H^1(\Omega)/\mathbb{R}}\mu(w)^2+\gamma(v_{\mathrm{MP2}})^2.\end{aligned}$$

All of them are guaranteed upper bounds of $|||\mathbf{u}-\mathbf{u}_h|||_{\mathrm{NC}}$ for the modified Crouzeix-Raviart finite element method (11) for $\boldsymbol{\pi}^{\mathrm{div}}=\boldsymbol{\pi}^{\mathrm{RT}}$ in the sense of Theorem 2.

Remark 4. *Compared to the Stokes problem, the minimisation problem for* w *is only a scalar elliptic conforming problem and therefore much cheaper to solve even for* $k=2$. *However, it might be a good idea to prolongate and update* w *from level to level by a truncated iterative solver.*

Remark 5. *The factor* $\|\mathbf{f}-\nabla w\|_{L^2(\Omega)}/\|\mathbf{f}\|_{L^2(\Omega)}$ *may be used to measure the divergence-free part of* $\mathbf{f}$ *and yields a criterion to decide if the modified Crouzeix-Raviart finite element method (when the factor is small) or the standard Crouzeix-Raviart finite element method (when the factor is close to* 1*) should be used.*

5. Numerical rxamples

5.1. **Adaptive mesh refinement algorithm.** The adaptive mesh refinement algorithm specified in Algorithm 2 with *red-green-blue*-refinement according to [Car04, Ver13] is steered by refinement indicators that are based on the a posteriori error estimators as follows. Given designs of $\mathbf{v}$ and w, the refinement indicators for the modified Crouzeix-Raviart finite element method (11) with $\boldsymbol{\pi}^{\mathrm{div}} = \boldsymbol{\pi}^{\mathrm{RT}}$ read, for all $T \in \mathcal{T}$,

$$\eta(T)^2 := C_F^2 \big\|\nu^{-1/2} h_T(\mathbf{f} - \nabla w)\big\|_{L^2(T)}^2 + \big\|\nu^{1/2}\nabla_h(\mathbf{u}_h - \mathbf{v})\big\|_{L^2(T)}^2 + c_0^{-2}\,\big\|\nu^{1/2}\,\mathrm{div}\,\mathbf{v}\big\|_{L^2(T)}^2,$$

while the the refinement indicators for the standard Crouzeix-Raviart finite element method (11) with $\boldsymbol{\pi}^{\mathrm{div}} = \boldsymbol{\pi}^{\mathrm{CR}}$ read, for all $T \in \mathcal{T}$,

$$\begin{aligned}\eta(T)^2 := \big\|\nu^{-1/2}\mathbf{f}_T/2 \otimes (\bullet - \mathrm{mid}(T))\big\|_{L^2(T)}^2 + C_P(T)^2\,\mathrm{osc}(\nu^{-1/2}\mathbf{f}, T)^2 \\ + \big\|\nu^{1/2}\nabla_h(\mathbf{u}_h - \mathbf{v})\big\|_{L^2(T)}^2 + c_0^{-2}\,\big\|\nu^{1/2}\,\mathrm{div}\,\mathbf{v}\big\|_{L^2(T)}^2.\end{aligned}$$

All experiments are performed on triangulations with rectangular triangles and the constants $C_F = 0.6215$ and $C_P(T) = 0.2610$. The inf-sup constant c_0 depends on the domain and is chosen problem-dependent. The bulk parameter Θ in Algorithm 2 is set to $\Theta = 0.5$ for adaptive mesh refinement or $\Theta = 1.0$ for uniform mesh refinement.

Algorithm 2: Adaptive mesh refinement algorithm

Input : Initial mesh $\mathcal{T}_0$ and $0 < \Theta \leq 1$
Output: Sequence of meshes $T_0, T_1, \ldots$
for $\ell = 0, 1, 2, \ldots$ *until termination* **do**
  Compute discrete solution u_h of (11) on $\mathcal{T}_\ell$
  Estimate and calculate refinement indicators $\eta(T)^2$
  Mark a minimal subset $\mathcal{M}_\ell$ of $\mathcal{T}_\ell$ such that $\Theta \sum_{T\in\mathcal{T}_\ell} \eta(T)^2 \leq \sum_{T\in\mathcal{M}_\ell} \eta(T)^2$
  Refine $\mathcal{T}_\ell$ by *red*-refinement of triangles in $\mathcal{M}_\ell$ and *red-green-blue*-refinement of further triangles to avoid hanging nodes and compute $\mathcal{T}_{\ell+1}$
end

5.2. **Example with rotation-free right hand side.** The first example considers a rotation-free right hand side $\mathbf{f} \equiv \nabla p$ for the exact pressure $p(x, y) = x^3 + y^3 - 0.5$ and zero velocity $\mathbf{u} \equiv 0$ on the unit square with inf-sup constant $c_0 = 0.3826$.

A rotation-free right hand side is the worst case for the standard Crouzeix-Raviart finite element method in the sense that the velocity, though an element of the ansatz space, cannot be found exactly due to the nonphysical interactions with the (only) discretely divergence-free test functions. Nevertheless, the energy error of the velocity can be estimated very sharply by the a posteriori error estimators as depicted in Figure 1.

The modified Crouzeix-Raviart finite element method computes the exact velocity solution and therefore the energy error is zero. Consequently, the second part of the error estimator vanishes for $\mathbf{v} \equiv 0$, i.e. $\gamma(0) = 0$. The $\mu(w)$ part in the error estimator would vanish for $w = p \in P_3(\Omega)$ in this example, but this choice is not possible for the error estimators η_{MP1}, η_{MP1RED} and η_{MP2}. However, $\mu(w)$ converges to zero with a higher converge rate than the energy error for the standard method as can be seen in Figure 1.

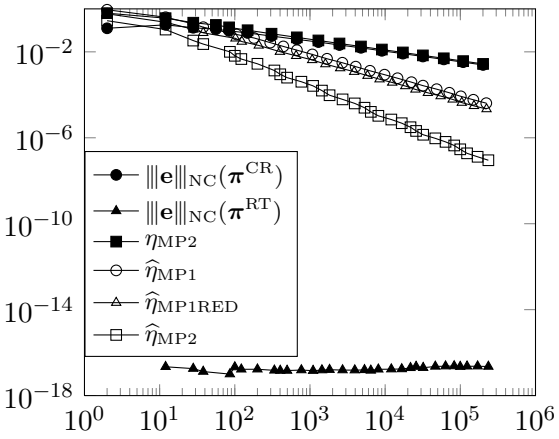

FIGURE 1. Convergence history of the exact energy error and the error estimators η_{MP2}, $\widehat{\eta}_{\mathrm{MP1}}$, $\widehat{\eta}_{\mathrm{MP1RED}}$ and $\widehat{\eta}_{\mathrm{MP2}}$ for adaptive mesh refinement in Subsection 5.2.

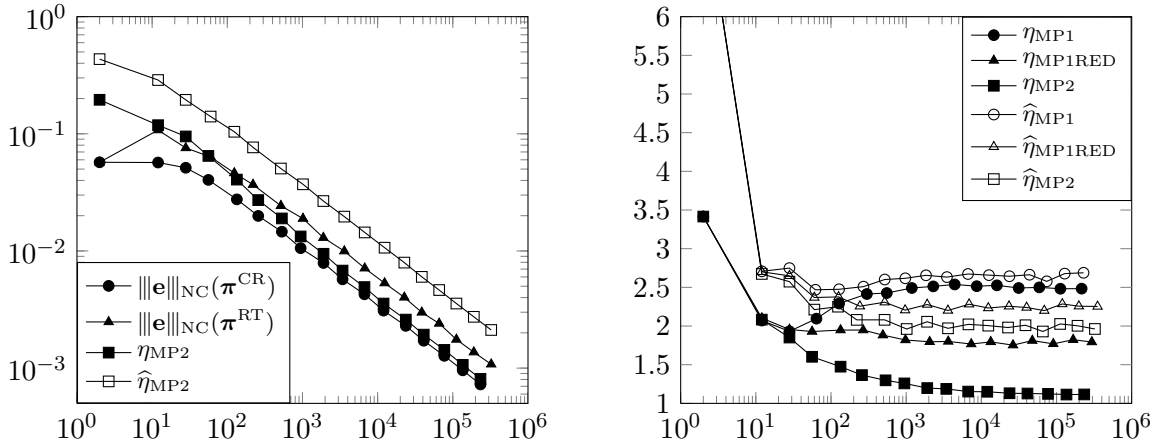

FIGURE 2. Convergence history of the exact energy error and the best error estimators (left) and efficiency indices $\eta/|||u-u_h|||_{\mathrm{NC}}$ of all error estimators η (right) for adaptive mesh refinement in Subsection 5.3.

5.3. **Example with zero pressure.** The second example considers the Stokes problem with $\mathbf{f} := -\Delta\mathbf{u}$ for the exact solution $\mathbf{u}(x,y) = \mathrm{rot}(x^2(1-x)^2y^2(1-y)^2)$, $\nu = 1$ and $p \equiv 0$ on the unit square with inf-sup constant $c_0 = 0.3826$.

Since the pressure is zero, the pressure-dependent error part of the standard method is zero and there is no pollution of the velocity error. In this worst case for the modified method, the energy error of the velocity solution of the modified version is slightly larger than the energy error in the standard method as depicted in Figure 2 for adaptive mesh refinement (the results for uniform mesh refinement are very similar). The efficiency index of $\widehat{\eta}_{\mathrm{MP2}}$ is about 2.0, while the efficiency index of η_{MP2} is about 1.1. A possible reason may be the constant of the Fortin interpolation operator in the contribution $\mu(w)$. A smaller (guaranteed lower bound of the) constant would lead to better efficiency indices. A similar but milder difference can be observed for the other estimators. The estimators η_{MP1RED} and $\widehat{\eta}_{\mathrm{MP1RED}}$ attain efficiency indices around 1.8 and 2.3, respectively, while η_{MP1} and $\widehat{\eta}_{\mathrm{MP1}}$ end up with efficiency indices about 2.5 vs. 2.7.

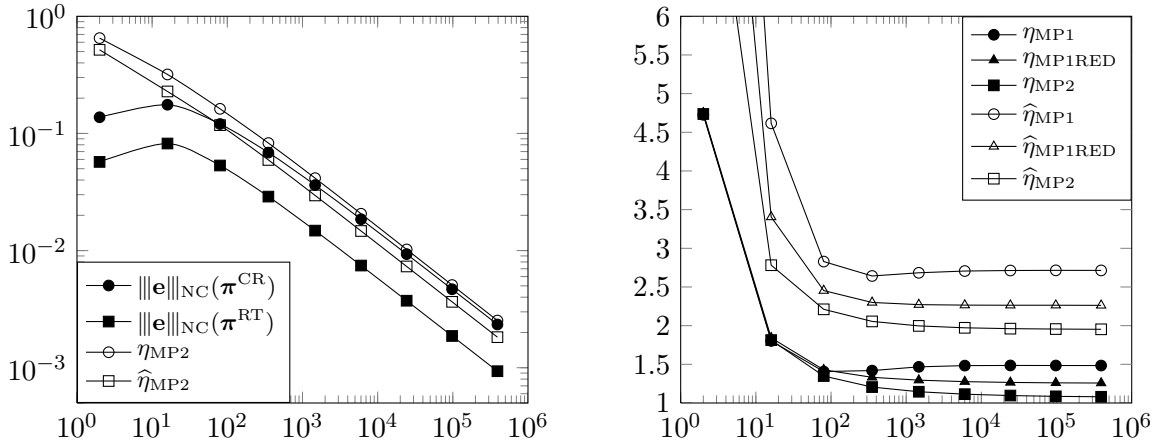

FIGURE 3. Convergence history of the exact energy error and the best error estimators (left) and efficiency indices $\eta/|||u-u_h|||_{\mathrm{NC}}$ of all error estimators η (right) for uniform mesh refinement in Subsection 5.4.

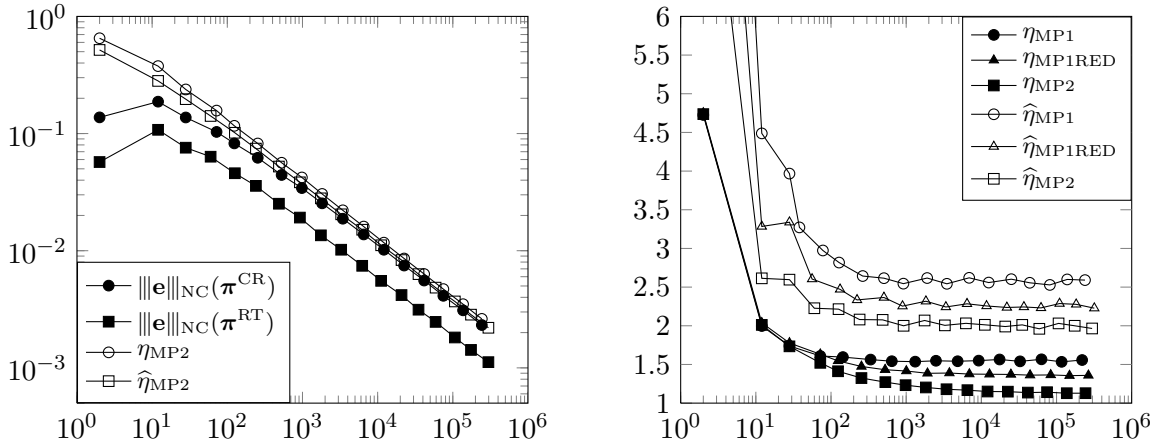

FIGURE 4. Convergence history of the exact energy error and the best error estimators (left) and efficiency indices $\eta/|||u-u_h|||_{\mathrm{NC}}$ of all error estimators η (right) for adaptive mesh refinement in Subsection 5.4.

5.4. **Example with smooth solution on unit square.** The third example considers the Stokes problem for the exact solution $\mathbf{u}(x,y) = \mathrm{rot}(x^2(1-x)^2y^2(1-y)^2)$ and $p(x,y) = x^3+y^3-0.5$ on the unit square for the right-hand side $\mathbf{f} := -\nu\Delta\mathbf{u} + \nabla p$ for $\nu = 1$. For the estimator we set $c_0 = 0.3826$.

The left part of Figures 3 and 4 show the convergence history for the exact energy errors of the standard and the modified Crouzeix-Raviart finite element method for uniform and adaptive refinement. The energy error for the modified method is smaller than the energy error for the standard method. Note, that for smaller ν the superiority of the modified method can be driven to an arbitrary extent. The figures also show the best guaranteed upper bounds for each method. While η_{MP2} for the standard method is very close to the exact energy error, the upper bound $\widehat{\eta}_{\mathrm{MP2}}$ for the modified method is not as efficient on coarse meshes due to the inexact approximation of α in (20). The convergence speed of the higher-order approximation error is significantly faster and restores the best efficiency at

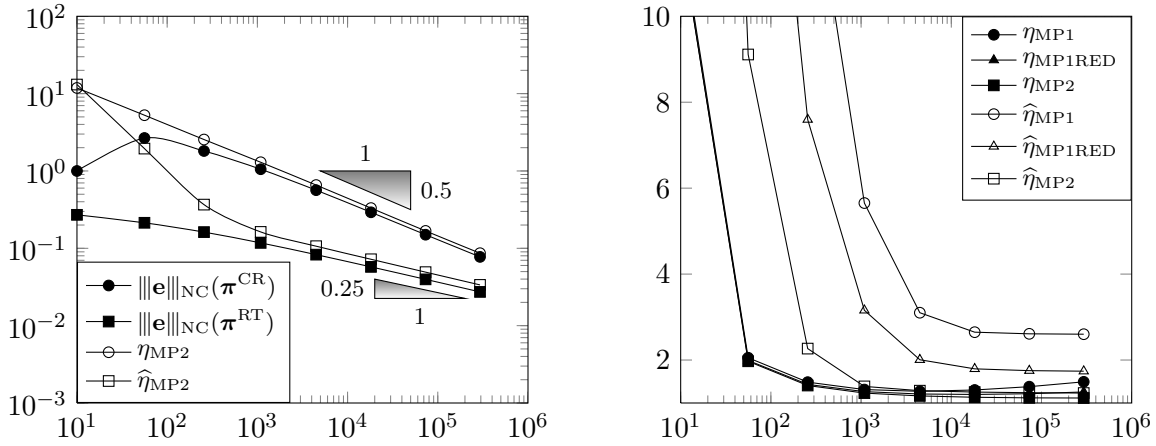

FIGURE 5. Convergence history of the exact energy error and the best error estimators (left) and efficiency indices $\eta/|||u-u_h|||_{\mathrm{NC}}$ of all error estimators η (right) for uniform mesh refinement in Subsection 5.5.

around 10^3 degrees of freedom. Then, the efficiency index of $\widehat{\eta}_{\mathrm{MP2}}$ is about 2.0. The other estimators for the modified method $\widehat{\eta}_{\mathrm{MP1RED}}$ and η_{MP1} attain slithly worse efficiency indices between 2.2 and 2.7 as depicted in the right part of Figures 3 and 4.

5.5. **Example with smooth solution on L-shaped domain.** The last example studies $f \equiv \nabla p$ for the pressure $p(x,y) = 100\sin(xy\pi)$ on the L-shaped domain $\Omega = (-1,1)^2 \setminus ((0,1)\times(-1,0))$ with the exact velocity solution

$$\mathbf{u}(r,\varphi) = r^\alpha \begin{pmatrix} (\alpha+1)\sin(\varphi)\psi(\varphi) + \cos(\varphi)\psi'(\varphi) \\ -(\alpha+1)\cos(\varphi)\psi(\varphi) + \sin(\varphi)\psi'(\varphi) \end{pmatrix}^T$$

given in polar coordinates and with

$$\psi(\varphi) = 1/(\alpha+1)\,\sin((\alpha+1)\varphi)\cos(\alpha\omega) - \cos((\alpha+1)\varphi) \\ + 1/(\alpha-1)\,\sin((\alpha-1)\varphi)\cos(\alpha\omega) + \cos((\alpha-1)\varphi)$$

and $\alpha = 856399/1572864 \approx 0.54$, $\omega = 3\pi/2$ from [Ver89]. For the estimator we set $c_0 = 0.3$.

Figure 5 shows the convergence history for uniform mesh refinement, while Figure 6 shows the convergence history for adaptive mesh refinement. The reconstructed method ($\boldsymbol{\pi}^{\mathrm{RT}}$) has a convergence rate of about 0.25 with respect to the number of degrees of freedom for uniform mesh refinement, whereas the standard method ($\boldsymbol{\pi}^{\mathrm{CR}}$) seems to have the optimal convergence rate of 0.5 which corresponds to a convergence of $O(h)$ in two dimensions. This might be the influence of the dominating pressure contribution in the a priori energy estimate that pollutes the overall energy error but decreases faster than the contribution from the exact velocity. However, even on the finest mesh the error of the standard method is still larger than the error of the modified method. With adaptive mesh refinement, all methods lead to optimal convergence rates and the modified method preserves its headstart of an more than one magnitude smaller energy error. While the efficiency of $\widehat{\eta}_{\mathrm{MP1}}$ and $\widehat{\eta}_{\mathrm{MP1RED}}$ are slightly worse, the efficiency indices of $\widehat{\eta}_{\mathrm{MP2}}$ are comparable with those of η_{MP2}. Due to the inexact approximation of α in (20), there is an preasymptotic phase with suboptimal efficiency indices that ends at around 10^3 degrees of freedom for $\widehat{\eta}_{\mathrm{MP2}}$ and around 10^4 degrees of freedom for $\widehat{\eta}_{\mathrm{MP1}}$ and $\widehat{\eta}_{\mathrm{MP1RED}}$. However, the guaranteed upper bounds for the energy error always remain below the energy error for the standard method after 100 degrees of

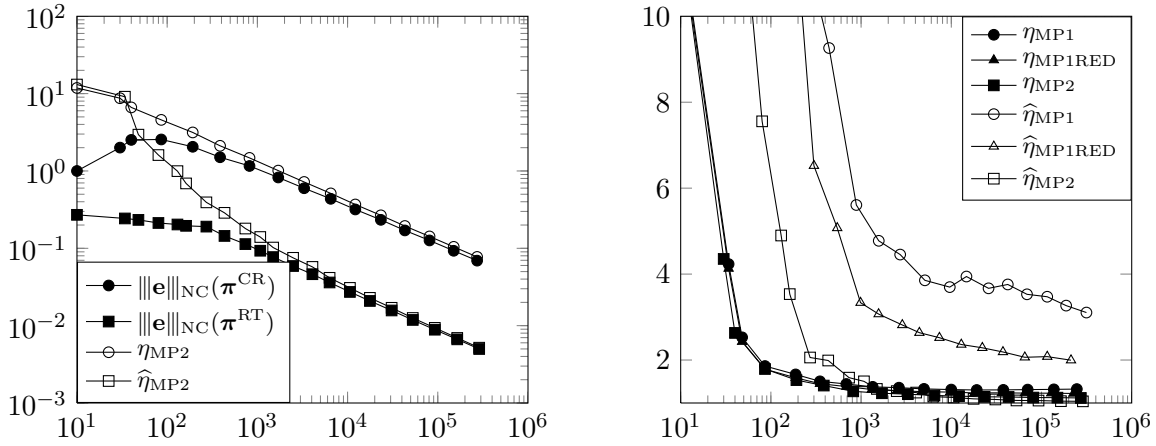

FIGURE 6. Convergence history of the exact energy error and the best error estimators (left) and efficiency indices $\eta/|||u - u_h|||_{\mathrm{NC}}$ of all error estimators η (right) for adaptive mesh refinement in Subsection 5.5.

freedom. The availability of such a guaranteed upper bound increases the interest in the modified method with divergence-free reconstructions of the test functions.

REFERENCES

[AD99] G. Acosta and R. G. Durán, *The maximum angle condition for mixed and nonconforming elements: application to the Stokes equations*, SIAM J. Numer. Anal. **37** (1999), no. 1, 18–36 (electronic). MR 1721268 (2000g:65107)

[Ago94] A. Agouzal, *A posteriori error estimator for nonconforming finite element methods*, Appl. Math. Lett. **7** (1994), no. 5, 61–66.

[Ain04] Mark Ainsworth, *Robust a posteriori error estimation for nonconforming finite element approximation*, SIAM J. Numer. Anal. **42** (2004), no. 6, 2320–2341.

[Beb03] M. Bebendorf, *A note on the Poincaré inequality for convex domains*, Z. Anal. Anwendungen **22** (2003), no. 4, 751–756.

[BF91] Franco Brezzi and Michel Fortin, *Mixed and hybrid finite element methods*, Springer-Verlag New York, Inc., New York, NY, USA, 1991.

[BLMS14] C. Brennecke, A. Linke, C. Merdon, and J. Schöberl, *Optimal and pressure-independent L^2 velocity error estimates for a modified Crouzeix-Raviart Stokes element with BDM reconstructions*, WIAS Preprint (2014), no. 1929.

[BW91] R. E. Bank and B. D. Welfert, *A posteriori error estimates for the Stokes problem*, SIAM J. Numer. Anal. **28** (1991), no. 3, 591–623.

[Car04] Carsten Carstensen, *An adaptive mesh-refining algorithm allowing for an H^1 stable L^2 projection onto Courant finite element spaces*, Constr. Approx. **20** (2004), no. 4, 549–564. MR 2078085 (2005i:65182)

[CGR12] Carsten Carstensen, Joscha Gedicke, and Donsub Rim, *Explicit error estimates for Courant, Crouzeix-Raviart and Raviart-Thomas finite element methods*, J. Comput. Math. **30** (2012), no. 4, 337–353. MR 2965987

[CM14] Carsten Carstensen and Christian Merdon, *Computational Survey on A Posteriori Error Estimators for the Crouzeix–Raviart Nonconforming Finite Element Method for the Stokes Problem*, Comput. Methods Appl. Math. **14** (2014), no. 1, 35–54. MR 3149616

[CR73] M. Crouzeix and P.-A. Raviart, *Conforming and nonconforming finite element methods for solving the stationary Stokes equations. I*, Rev. Française Automat. Informat. Recherche Opérationnelle Sér. Rouge **7** (1973), no. R-3, 33–75. MR 0343661 (49 #8401)

[DA05] W. Dörfler and M. Ainsworth, *Reliable a posteriori error control for nonconformal finite element approximation of Stokes flow*, Math. Comp. **74** (2005), no. 252, 1599–1619 (electronic).

[DM98] Philippe Destuynder and Brigitte Métivet, *Explicit error bounds for a nonconforming finite element method*, SIAM J. Numer. Anal. **35** (1998), no. 5, 2099–2115 (electronic).

[Gal94] G. P. Galdi, *An introduction to the mathematical theory of the Navier-Stokes equations. Vol. II*, Springer Tracts in Natural Philosophy, vol. 39, Springer-Verlag, New York, 1994, Nonlinear steady problems. MR 1284206 (95i:35216b)

[GR86] V. Girault and P.-A. Raviart, *Finite element methods for Navier-Stokes equations*, Springer Series in Computational Mathematics, vol. 5, Springer-Verlag, Berlin, 1986.

[Lin14] Alexander Linke, *On the role of the Helmholtz decomposition in mixed methods for incompressible flows and a new variational crime*, Comput. Methods Appl. Mech. Engrg. **268** (2014), 782–800. MR 3133522

[LS10] R. S. Laugesen and B. A. Siudeja, *Minimizing Neumann fundamental tones of triangles: an optimal Poincaré inequality*, J. Differential Equations **249** (2010), no. 1, 118–135. MR 2644129 (2011f:35238)

[PW60] L.E. Payne and H.F. Weinberger, *An optimal poincar inequality for convex domains*, Archive for Rational Mechanics and Analysis **5** (1960), no. 1, 286–292 (English).

[Tem91] R. Temam, *Navier-Stokes equations*, Elsevier, North-Holland, 1991.

[Ver89] R. Verfürth, *A posteriori error estimators for the Stokes equations*, Numer. Math. **55** (1989), no. 3, 309–325.

[Ver13] Rüdiger Verfürth, *A posteriori error estimation techniques for finite element methods*, Numerical Mathematics and Scientific Computation, Oxford University Press, Oxford, 2013. MR 3059294

[VHS11] M. Vohralík, A. Hannukainen, and R. Stenberg, *A unified framework for aposteriori error estimation for the stokes problem*, Accepted for Numer. Math. (2011), HAL Preprint 00470131, http://hal.archives–ouvertes.fr/hal–00470131/en/.